Level statistics and eigenfunctions of square torus billiards: Manifesting the transition from regular to chaotic behaviors

P. H. Tuan, Y. T. Yu, P. Y. Chiang, H. C. Liang, K. F. Huang, and Y. F. Chen*

Department of Electrophysics, National Chiao Tung University, 1001 Ta-Hsueh Road, Hsinchu 30010, Taiwan

(Received 27 November 2011; revised manuscript received 16 January 2012; published 2 February 2012)

We thoroughly analyze the level statistics and eigenfunctions in concentric as well as nonconcentric square torus billiards. We confirm the characteristics of quantum and classical correspondence and the existence of scarred and superscarred modes in concentric square torus billiards. Furthermore, we not only verify that the transition from regular to chaotic behaviors can be manifested in nonconcentric square torus billiards, but also develop an analytical distribution to excellently fit the numerical level statistics. Finally, we intriguingly observe that numerous eigenstates commonly exhibit the wave patterns to be an ensemble of classical diamond trajectories, as the effective wavelengths are considerably shorter than the size of internal hole.

DOI: 10.1103/PhysRevE.85.026202 PACS number(s): 05.45.Mt, 03.65.Ge

I. INTRODUCTION

Two-dimensional billiards has long been a useful tool for studying quantum chaos issues due to its simplicity [1,2]. The dynamical behaviors, from the most regular (integrable) to the most chaotic (nonintegrable), are found to depend on the geometry of the billiard boundary. The integrable systems with classical trajectories confined to an invariant torus in phase space display the Poisson distribution in level spacing statistics [3]. In contrast, the nonintegrable systems with ergodic trajectories have been verified to obey the Wigner statistics of level spacing [4]. Besides the two extreme classes, there is a diverse category called pseudointegrable systems whose phase space trajectories are not fully ergodic but are bounded on invariant multihandled spheres (topological structure with genus $2 \leqslant g < \infty$) [5–7]. Pseudointegrable billiards, such as rational polygons, staircase billiards, and integrable billiards with singular scatter inside, have been widely explored in the last few decades [8–13]. It was found that the energy spectra in pseudointegrable systems could reveal intermediate cases between integrable and chaotic ones [12,14,15]. The existence of intermediate cases attracts considerable attention with regard to investigating the transition between the two limiting behaviors. It has been verified that there is a systematic change from Poisson-like toward Wigner-like behavior with increasing the genus number in pseudointegrable systems [16–18]. To the best of our knowledge, the exploration for the continuous transition between integrable and chaotic behaviors for the pseudointegrable system with a fixed genus number has not been performed in depth.

Square torus billiards, a genus 5 pseudointegrable system with special geometry similar to the Sinai billiard, has the potential to explore field chaos problems in the coaxial waveguide [19,20]. It was found [6] that the eigenenergies of eighth square torus billiards exhibit the level repulsion phenomenon with level statistics lying between Poisson and Wigner distributions. This finding leads us to conjecture whether nonconcentric square torus billiards is a paradigm system with a fixed genus number for exploring the transition between integrable and chaotic behaviors. Nonconcentric square torus billiards means that the position of the internal square hole deviates from the center of the external square boundary.

In this work we perform thorough numerical analyses to verify that the level statistics of nonconcentric square torus billiards can manifest the transition between integrable and chaotic behaviors. We first analyze the level statistics and eigenfunctions of concentric square torus billiards to confirm the validity of the numerical computation based on the expansion method [21,22]. The Fourier-transformed length spectrum of numerical energy levels is clearly found to reveal quantum and classical correspondence. The scarred and superscarred modes [23–25] are noticeably observed to further validate the numerical analysis. We then employ the same numerical method to analyze the level statistics and eigenfunctions of nonconcentric square torus billiards. It is found that the transition from regular to chaotic behaviors can be manifested with continuously offsetting the position of the internal square hole. The transition property can be further confirmed from the Fourier-transformed length spectra. Finally, we systematically explore the morphologies of eigenfunctions from low-order to very high-order eigenstates for nonconcentric square torus billiards with different offsetting conditions. We observed that when the effective wavelengths are considerably shorter than the hole size, numerous eigenstates commonly exhibit the wave patterns to be an ensemble of classical diamond trajectories, independent of offsetting conditions.

II. CONCENTRIC SQUARE TORUS BILLIARDS

Rational polygon billiards is a system with only rational interior angles $n_i\pi/m_i$, where $n_i, m_i \in N$ and at least one $n_i > 1$. For this kind of pseudointegrable billiards, the genus number can be described by [6,26]

$$g = 1 + \frac{M}{2}\sum_{i=1}^{J}\frac{n_i - 1}{m_i}, \tag{1}$$

where J is the number of interior angles and M is the least common multiple of m_i. Figure 1(a) shows the geometry of square torus billiards whose side-length of outer square boundary and inner square hole are a and b, respectively. According to Eq. (1), square torus billiards with eight rational interior angles (four equal to $\pi/2$and four equal to $3\pi/2$) can

*yfchen@cc.nctu.edu.tw

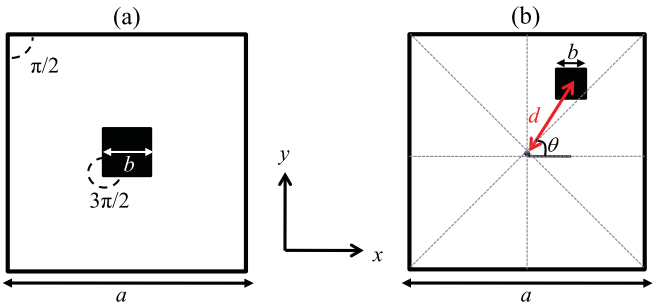

FIG. 1. (Color online) Geometries of (a) concentric square torus billiards and (b) nonconcentric square torus billiards.

be classified as genus 5 with phase space to be a five-handled sphere. We exploit the expansion method [22] to calculate the eigenenergies and eigenfunctions of square torus billiards. Since the matrix elements of the Hamilton can be analytically expressed with the help of eigenstates $\phi_m(\vec{r})$ of square billiards, only a few minutes are taken to obtain about 2000 reliable energy levels by a conventional personal computer.

We give a brief synopsis for the expansion method as follows. The time-independent Schrödinger equation for billiard problems can be written as $\hat{H}\psi_n(\vec{r}) = E_n\psi_n(\vec{r})$, where E_n is the eigenenergy and $\psi_n(\vec{r})$ is the eigenfunction of the Hamiltonian operator $\hat{H}$. With the help of eigenstates $\phi_m(\vec{r})$ of square billiards, the eigenfunction $\psi(\vec{r})$ for square torus billiards can be expanded as $\psi(\vec{r}) = \sum_m c_m\phi_m(\vec{r})$. By substituting this expression into the differential equation, we obtain a linear matrix problem of $H_{mn}c_m = Ec_n$ with matrix elements of $H_{mn} = H^0_{mn} + V_0 v_{mn}$, where H^0_{mn} is the matrix element of square billiards, V_0 is a sufficiently large constant to approximate the infinite potential of billiards, and v_{mn} is the matrix element to be associated with the geometry of billiards. The matrix element v_{mn} can be written as $v_{mn} = \int_\Omega d^2\phi^*_m(\vec{r})\phi_n(\vec{r})$, where Ω includes all regions with infinite potential. For square torus billiards, the matrix element v_{mn} is explicitly given by

$$v_{mn} = \left(\frac{2}{a}\right)^2 \left[\int_{(a-b)/2}^{(a+b)/2} \sin\left(\frac{m_1\pi x}{a}\right)\sin\left(\frac{m_2\pi x}{a}\right)dx\right] \times \left[\int_{(a-b)/2}^{(a+b)/2} \sin\left(\frac{n_1\pi y}{a}\right)\sin\left(\frac{n_2\pi y}{a}\right)dy\right], \quad (2)$$

where we denote $m = (m_1,m_2)$ and $n = (n_1,n_2)$. Since the matrix elements H_{mn} can be integrated analytically, the time consumption is significantly reduced in the calculation of eigenenergies and eigenfunctions.

The number of reliable eigenstates was found to be nearly 1850s when we used 2100 eigenstates of square billiards in the calculation. We employed the periodic orbit theory [2,27] to analyze the calculated energy spectra for confirming the accuracy of computation. According to the Gutzwiller trace formula, the characteristics of classical periodic orbits can be extracted from the Fourier-transformed spectra of the eigenvalue density:

$$\rho_{FT}(L) = \sum_{n=1}^{\infty}\int_{-\infty}^{\infty}\delta(k-k_n)e^{ikL}dk = \sum_{n=1}^{\infty}e^{ik_nL} = \sum_{n=1}^{\infty}\sum_{\mu}\rho_{\nu,\mu}\delta(L-\nu L_\mu), \quad (3)$$

where index μ labels the periodic orbits, and $\nu = 1,2,...$ run over all recurrences of such orbits. Equation (3) indicates that the Fourier length spectrum $\rho_{FT}(L)$ is formed by a series of intense peaks at multiples of the lengths of classical periodic orbits, i.e., at $L = \nu L_\mu$. For numerical evaluation, we substituted all the calculated energy levels into the expression $\rho_N(L) = \sum_{n=1}^{N} e^{ik_nL}$, where N is the total number of energy levels. Figure 2 depicts the Fourier length spectrum $|\rho_N(L)|^2$of a square torus billiard with $b = a/5$. It is clearly seen that there is a series of sharp peaks at the lengths corresponding to classical periodic orbits. We also investigated the eigenfunctions and confirmed the existence of superscarred [24,25] modes in the pseudointegrable system, as shown in Figs. 3(a)–3(c). To our surprise, an anomalous mode which is wave-function localized on unstable periodic orbit can also be observed in our square torus model, as seen in Fig. 3(d), so-called scarred modes [23]. Scarred and superscarred modes have been confirmed to play an important role in interpreting the lasing modes of microcavity lasers [28–30]. Besides, we found that the scarred mode indicated in Fig. 3(d) is one kind of diffractive orbit studied in semiclassical physics [31,32]. The diffractive effects of quantum waves may be important in analyzing the energy spectra of pseudointegrable systems. In our square torus model, the numerical wave functions associated with the diffractive orbits can be found; however, their

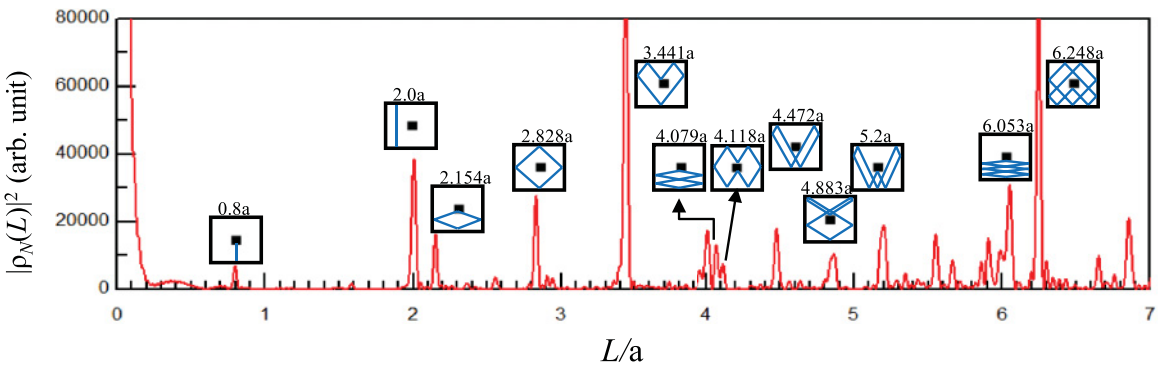

FIG. 2. (Color online) Fourier-transformed length spectrum $|\rho_N(L)|^2$for numerical energy levels of concentric square torus billiards with $b = a/5$. A series of intense peaks in accord with classical periodic orbits.

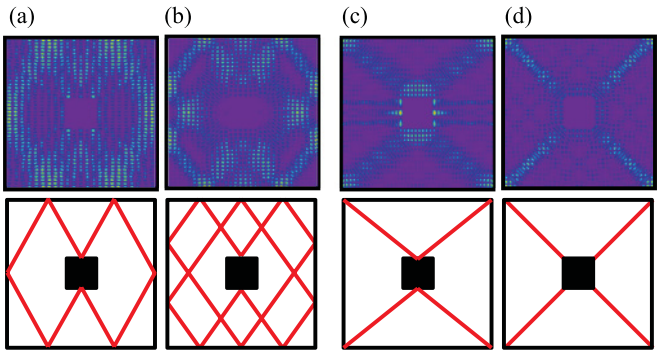

FIG. 3. (Color online) (a, b, c) Superscarred modes and (d) scarred mode observed in the eigenfunctions of concentric square torus billiards with $b = a/5$.

contribution to the characteristic length spectrum $|\rho_N(L)|^2$ is rather insignificant, as shown in Fig. 2.

Next, we analyzed the probability distribution of the normalized spacing $s_i = (E_{i+1} - E_i)/\langle s \rangle$ to investigate the level statistics, where $E_{i+1}$and E_i are two consecutive energy levels and $\langle s \rangle$ is the mean spacing. Figure 4 depicts the numerical histograms for the level spacing statistics. We also plot the Poisson distribution $p_P(s) = e^{-s}$ and the Wigner distribution $p_W(s) = (\pi s/2)\exp(-s^2\pi/4)$ in the same figure for comparison. It can be seen that the level statistics of concentric square torus billiards exhibit the level degeneracy phenomenon and are quite close to Poisson distribution. The level degeneracy mainly comes from the high symmetry along the three reflecting axes for square geometry, i.e., the horizontal, perpendicular, and diagonal lines passing the center of the outer square boundary. Next, we employ the same numerical method to explore how the level degeneracy is split by offsetting the internal square hole away from the center of the external square boundary.

III. NONCONCENTRIC SQUARE TORUS BILLIARDS

As shown in Fig. 1(b), nonconcentric square torus billiards can be completely specified by the size b and the location

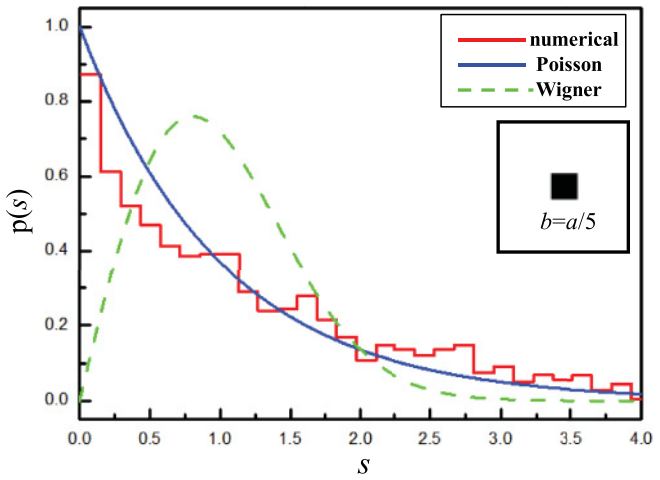

FIG. 4. (Color online) Level spacing statistics of concentric square torus billiards with $b = a/5$.

(d, θ) of the internal hole, where d is the offsetting distance from the center and θ is the offsetting direction with respect to the horizontal axis. It was numerically found that if the offsetting direction is along the symmetric axes of square torus, i.e., $\theta = 0, \pi/4$, and $\pi/2$, the level spacing statistics always display the Poisson distribution, independent of the size b and the offsetting distance d. In other words, the parameter θ plays a critical role in determining the basic property of level spacing statistics of nonconcentric square torus billiards. In contrast, as long as the offsetting direction θ deviates from the symmetric axes, the level spacing statistics is numerically found to gradually change from Poisson distribution toward Wigner-like distribution by increasing the offsetting distance d or increasing the size b.

Without loss of generality, we demonstrate the calculated results using the offsetting distance d as a variable for all cases with a fixed size b and a fixed direction θ. Hereafter, unless otherwise noted, the hole size and offsetting direction are fixed to be $b = a/5$ and $\theta = 3\pi/8$, respectively. Figure 5(a) depicts the level spacing statistics of nonconcentric square torus billiards for different offsetting distances (curves with histogram). It can be clearly seen that the level spacing statistics exhibit a conspicuous transition from regular to chaotic behavior with increasing the offsetting distance d. The value of $s_{\max}$, indicating the mean spacing for maximum probability of level statistics, clearly shifts from 0 to $2/\pi$, corresponding to the transition from Poisson to Wigner distribution. With the calculated energy levels we compute the Fourier-transformed length spectra $\rho_N(L)$ for all cases. As shown in Fig. 5(b), not only the amplitudes but also the total numbers for the resonant peaks prominently decrease with increasing the offsetting distance d. From a classical point of view, some of the stable periodic orbits originating by reflection on the central hole will be removed due to this kind of shift. Also, the shift may cause a large amount of periodic orbits in the square billiard to be blocked by the central hole. However, some of the family of stable periodic orbits will split into different classes with different lengths, as indicated in Fig. 5(b). For the case of $d = a/5$, only principal peaks corresponding to the bouncing-ball mode and the recurrence survive in the length spectrum. To be brief, both the level spacing statistics and the characteristic length spectra of nonconcentric square torus billiards noticeably display the continuous transition from regular to chaotic behavior.

An analytical distribution is practically useful for quantitatively describing the intermediate properties between regular and chaotic systems. Berry and Robnik [33] previously proposed an analytical formula formed by the superposition of Poisson and Wigner distributions:

$$p_{\mathrm{BR}}(s) = w(s)p_P(s) + [1 - w(s)]\, p_W(s), \tag{4}$$

where $w(s)$ is the weighting function derived from the phase space of the pseudointegrable system. Although the Berry-Robnik distribution can describe the variation from level clustering to level repelling for small spacing, it cannot precisely illustrate the $s_{\max}$ shifting of the numerical histograms shown in Fig. 5(a).

Lenz and Haake [34,35] also derived a distribution for the level statistics of pseudointegrable systems with

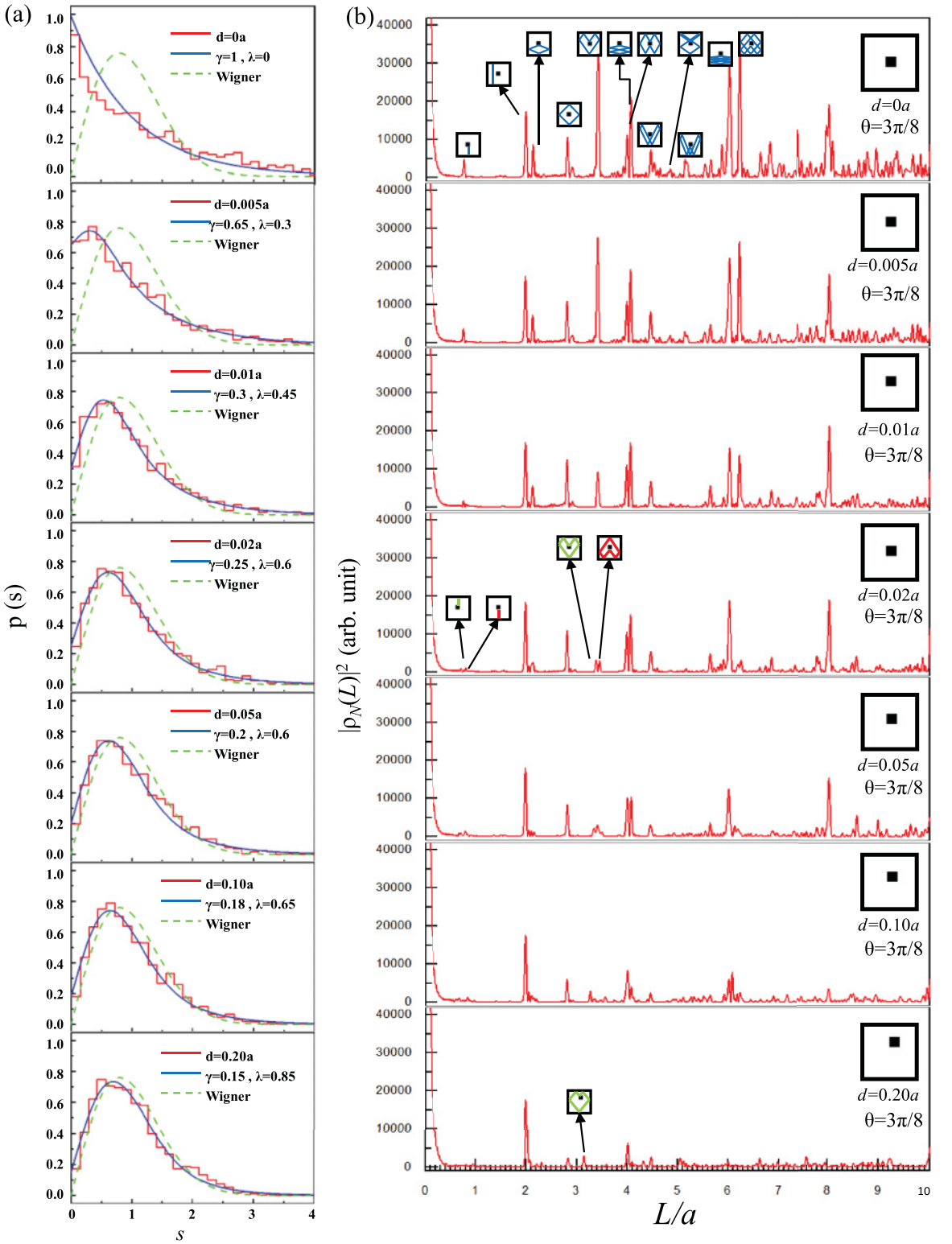

FIG. 5. (Color online) (a) Level spacing distribution: numerical statistics (histograms), analytical fitting distribution with Eq. (6) (solid line), and Wigner distribution (dashed line). (b) Fourier-transformed length spectra corresponding to each case in (a).

approximating the Hamiltonian as $H_\lambda = (1+\lambda^2)^{-1/2}(H_0 + \lambda V)$, where H_0 and V belong to Poisson and Gaussian orthogonal ensemble (GOE) contributions, respectively. The coupling coefficient λ can describe the system changing from regular to fully chaotic behavior by varying its value from 0 to ∞. The Lenz-Haake distribution is given by

$$p_{\mathrm{LH}}(s;\lambda) = \frac{u(\lambda)^2}{\lambda} s e^{-[u(\lambda)s/2\lambda]^2} \int_0^\infty e^{-(x^2+2x\lambda)} I_0(u(\lambda)xs/\lambda)dx \tag{5}$$

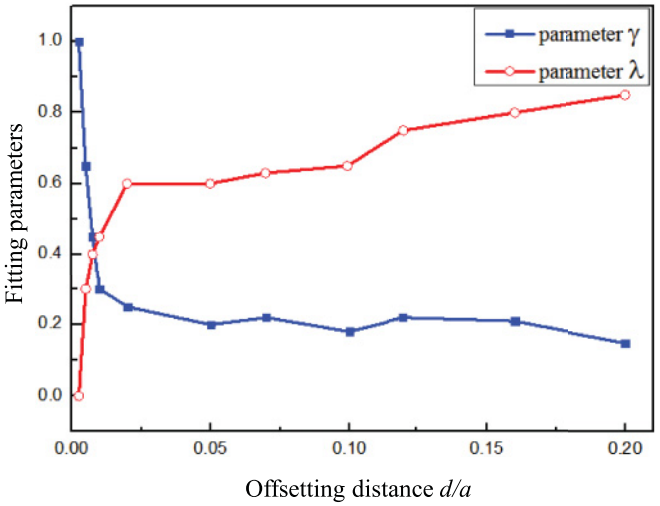

FIG. 6. (Color online) Dependence of the fitting parameters λ and γ on the offsetting distance d in nonconcentric square torus billiards.

with

$$u(\lambda) = \sqrt{\pi}U(-1/2,0,\lambda^2),$$

where $I_0(x)$ is the modified Bessel function and $U(a,b,x)$ is the Kummer function. We found that the Lenz-Haake distribution could fit the $s_{\max}$ shifting of level spacing statistics of nonconcentric square torus billiards. However, $p_{\mathrm{LH}}(0;\lambda)$ is always equal to zero for any $\lambda \neq 0$. Consequently, the Lenz-Haake distribution $p_{\mathrm{LH}}(s;\lambda)$ cannot characterize intermediate cases in the neighborhood of $s = 0$ very well .

We combine the Berry-Robnik and Lenz-Haake models to develop an analytical distribution in terms of $p_{\mathrm{BR}}(s)$ and $p_{\mathrm{LH}}(s;\lambda)$ for fitting the numerical histograms of nonconcentric square torus billiards:

$$p(s;\lambda,\gamma) = \gamma p_P(s) + (1-\gamma)p_{\mathrm{LH}}(s;\lambda), \qquad (6)$$

where γ is the weighting parameter for characterizing the detailed structure of level spacing statistics. Note that the parameter λ in $p_{\mathrm{LH}}(s;\lambda)$ mainly exemplifies the peak position of level spacing statistics. As shown in Fig. 5(a), the distribution $p(s;\lambda,\gamma)$ in Eq. (6) can fit the numerical histograms of level spacing statistics very well. Figure 6 depicts the dependence of parameters λ and γ on the offsetting distance d to quantitatively manifest the rate of transition from regular to chaotic properties. It can be seen that there is an abrupt change for both parameters λ and γ in the region of small offsetting distance $d = 0 \sim 0.02a$. In contrast, both γ and λ evolve smoothly for the offsetting distance d greater than $0.02a$. These results confirm that nonconcentric square torus billiards is an excellent pseudointegrable system for revealing the continuous transition between regular and chaotic behaviors without changing the genus number.

Furthermore, we investigate the morphologies of eigenfunctions of nonconcentric square torus billiards. We select two representative cases with a hole size of $b = a/10$ for illustration, one with a small offsetting distance of $d = 0.054a$ and the other with a relatively large distance of $d = 0.224a$.

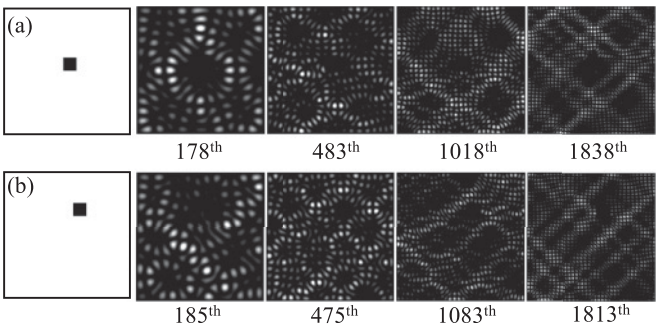

FIG. 7. Wave patterns from low-order to high-order eigenstates for nonconcentric square torus billiards with a hole size of $b = a/10$ under two different offsetting conditions: (a) $d = 0.054a$ and (b) $d = 0.224a$.

Figure 7 shows the typical wave patterns of the two cases for different orders ranging from hundreds to thousands. For the eigenstates with order between the 100th and 300th states, the wave patterns of the case with $d = 0.054a$ are found to be similar to the symmetric and regular morphologies of the eigenstates in concentric square torus billiards. On the other hand, the wave patterns of the case with $d = 0.224a$ are found to be quite irregular because of a greater symmetry breaking. For the eigenstates with order between the 400th and 1100th states, the wave patterns are found to display rather disordered morphologies. For the eigenstates with order greater than the 1800th state, the effective wavelengths are conspicuously shorter than the hole size and the wave patterns of numerous states are found to exhibit an ensemble of classical diamond trajectories, as seen in Fig. 7. This intriguing feature of particlelike trajectories reveals the importance of the comparison between the effective wavelength of eigenstates and the hole size of the billiards.

Finally, it is worthwhile to mention that the energy spectra may be obtained from the periodic orbits and the length spectra. Although this approach is somehow more intricate, it has been performed for several systems [36–39]. In principle, a similar procedure is possible to obtain the energy spectra for the square torus model. However, the current difficulty is to establish a relationship between the periodic orbits and the offsetting distance d.

IV. CONCLUSIONS

We have thoroughly analyzed level statistics and eigenfunctions for square torus billiards to explore the quantum and classical correspondence and the transition between integrable and chaotic behaviors. For concentric square torus billiards, we not only confirmed the Fourier-transformed length spectrum of numerical energy levels to clearly display the characteristics of quantum and classical correspondence, but we also observed the existence of scarred and superscarred modes. For nonconcentric square torus billiards, we verified that the transition from regular to chaotic behaviors can be manifested with continuously offsetting the position of the internal square hole. The transition property can be revealed as well from the Fourier-transformed length spectra. We also developed an analytical distribution to fit the numerical level statistics of nonconcentric square torus billiards in an excellent way. Finally, we observed

that numerous eigenstates commonly exhibit the wave patterns to be an ensemble of classical diamond trajectories when the effective wavelengths are considerably shorter than the hole size.

ACKNOWLEDGMENT

The authors acknowledge the National Science Council of Taiwan for their financial support of this research under Contract No. NSC-100-2628-M-009-001-MY3.

[1] H. J. Stöckmann, *Quantum Chaos–An Introduction* (Cambridge University Press, Cambridge, 1999).
[2] M. C. Gutzwiller, *Chaos in Classical and Quantum Mechanics* (Springer-Verlag, New York, 1990).
[3] M. V. Berry and M. Tabor, Proc. R. Soc. A **356**, 375 (1977).
[4] O. Bohigas, M. J. Giannoni, and C. Schmit, Phys. Rev. Lett. **52**, 1 (1984).
[5] A. N. Zemlyakov and A. B. Katok, Math. Notes **18**, 291 (1975).
[6] P. J. Richens and M. V. Berry, Physica D **2**, 495 (1981).
[7] K. Życzkowski, Acta Phys. Pol. B **23**, 245 (1992).
[8] T. Cheon and T. D. Cohen, Phys. Rev. Lett. **62**, 2769 (1989).
[9] D. Biswas and S. R. Jain, Phys. Rev. A **42**, 3170 (1990).
[10] A. Shudo and Y. Shimizu, Phys. Rev. E **47**, 54 (1993).
[11] P. Šeba and K. Życzkowski, Phys. Rev. A **44**, 3457 (1991).
[12] T. Shigehara, N. Yoshinaga, T. Cheon, and T. Mizusaki, Phys. Rev. E **47**, R3822 (1993).
[13] T. Shigehara, Phys. Rev. E **50**, 4357 (1994).
[14] T. Cheon, T. Mizusaki, T. Shigehara, and N. Yoshinaga, Phys. Rev. A **44**, R809 (1991).
[15] A. Shudo, Y. Shimizu, P. Šeba, J. Stein, H.-J. Stöckmann, and K. Życzkowski, Phys. Rev. E **49**, 3748 (1994).
[16] S. Russ, Phys. Rev. E **64**, 056240 (2001).
[17] Y. Hlushchuk and S. Russ, Phys. Rev. E **68**, 016203 (2003).
[18] J. Sakhr and J. M. Nieminen, Phys. Rev. E **72**, 045204(R) (2005).
[19] A. S. Omar and K. F. Schünemann, IEEE Trans. Microwave Theory Tech. **39**, 944 (1991).
[20] R. L. Liboff and J. Liu, Chaos **10**, 756 (2000).
[21] T. Shigehara and T. Cheon, Phys. Rev. E **54**, 1321 (1996).
[22] D. L. Kaufman, I. Kosztin, and K. Schulten, Am. J. Phys. **67**, 133 (1999).
[23] E. J. Heller, Phys. Rev. Lett. **53**, 1515 (1984).
[24] E. Bogomolny and C. Schmit, Phys. Rev. Lett. **92**, 244102 (2004).
[25] E. Bogomolny, B. Dietz, T. Friedrich, M. Miski-Oglu, A. Richter, F. Schäfer, and C. Schmit, Phys. Rev. Lett. **97**, 254102 (2006).
[26] E. Gutkin, Physica D **19**, 311 (1986).
[27] R. Balian and C. Bloch, Ann. Phys. (NY) **60**, 401 (1970); **64**, 271 (1971); **69**, 76 (1970); **85**, 514 (1974).
[28] R. C. C. Chen, Y. T. Yu, Y. J. Huang, C. C. Chen, Y. F. Chen, and K. F. Huang, Opt. Lett. **34**, 1810 (2009).
[29] K. F. Huang, Y. F. Chen, H. C. Lai, and Y. P. Lan, Phys. Rev. Lett. **89**, 224102 (2002).
[30] Y. F. Chen, Y. T. Yu, P. Y. Chiang, P. H. Tuan, Y. J. Huang, H. C. Liang, and K. F. Huang, Phys. Rev. E **83**, 016208 (2011).
[31] D. Biswas and S. Sinha, Phys. Rev. Lett. **70**, 916 (1993).
[32] G. Vattay, A. Wirzba, and P. E. Rosenqvist, Phys. Rev. Lett. **73**, 2304 (1994).
[33] M. V. Berry and M. Robnik, J. Phys. A **17**, 2413 (1984).
[34] G. Lenz and F. Haake, Phys. Rev. Lett. **65**, 2325 (1990).
[35] G. Lenz and F. Haake, Phys. Rev. Lett. **67**, 1 (1991).
[36] R. Aurich, M. Sieber, and F. Steiner, Phys. Rev. Lett. **61**, 483 (1988).
[37] M. Sieber and F. Steiner, Phys. Rev. Lett. **67**, 1941 (1991).
[38] R. Aurich and F. Steiner, Phys. Rev. A **45**, 583 (1992).
[39] S. Russ and J. Mellenthin, Phys. Rev. E **73**, 066227 (2006).